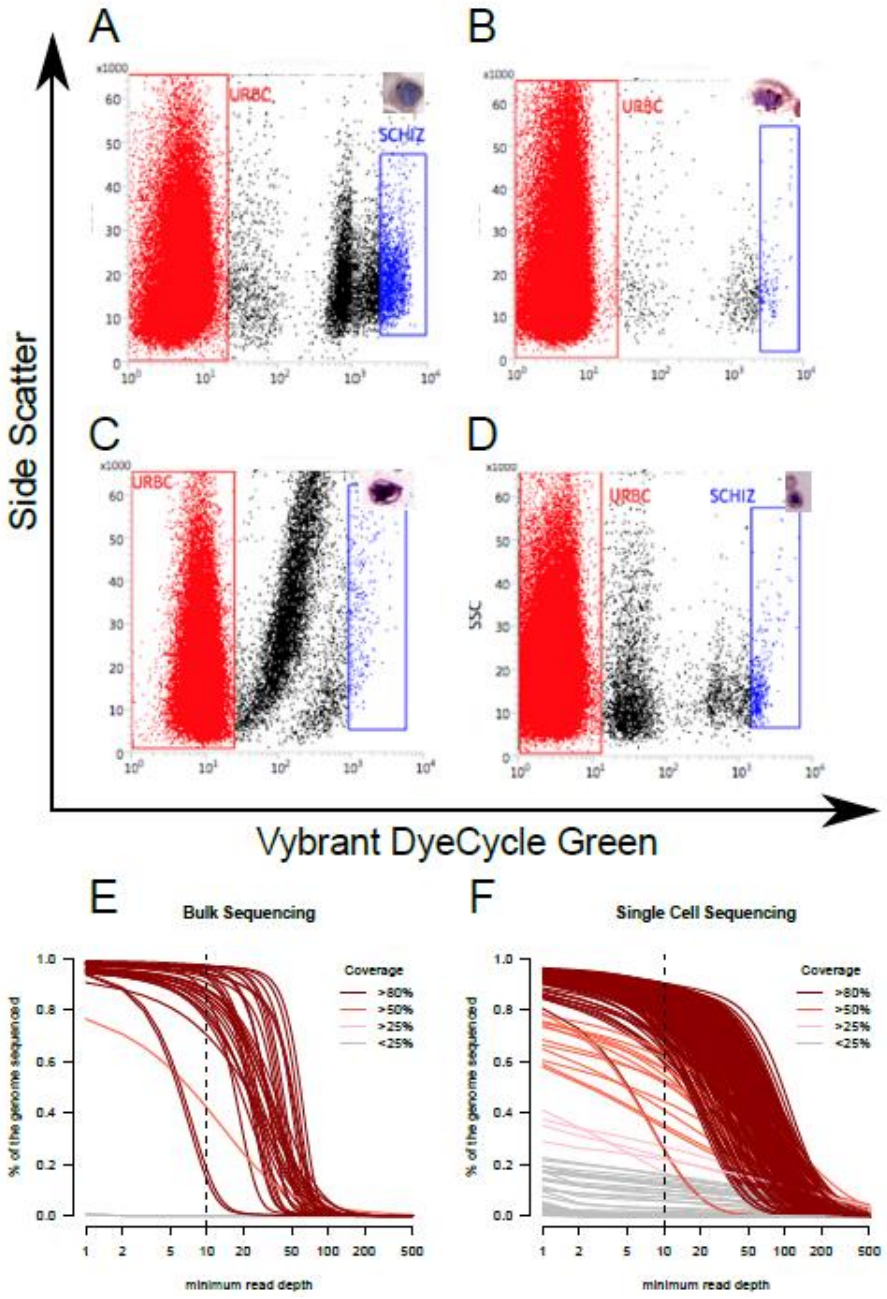

Fig. S1. Flow sorting and sequencing of single cells, related to Figure 1. (A-D) Representative FACS plots from four patient time points. FACS was performed after magnetic enrichment. Magnetic enrichment increases parasitaemia, and preferentially captures late stage parasites, however as they were present at high frequency in the infection there are substantial number of uninfected and early stage parasites remaining. In each plot the red box identifies uninfected red blood cells and the blue box represents the target cells for sorting. Read depth data from (E) bulk infections and (F) single cells. Each line shows the proportion of the genome covered by reads at increasing read depth thresholds. Data is colored by the proportion of the genome covered by at least 1X (legend).

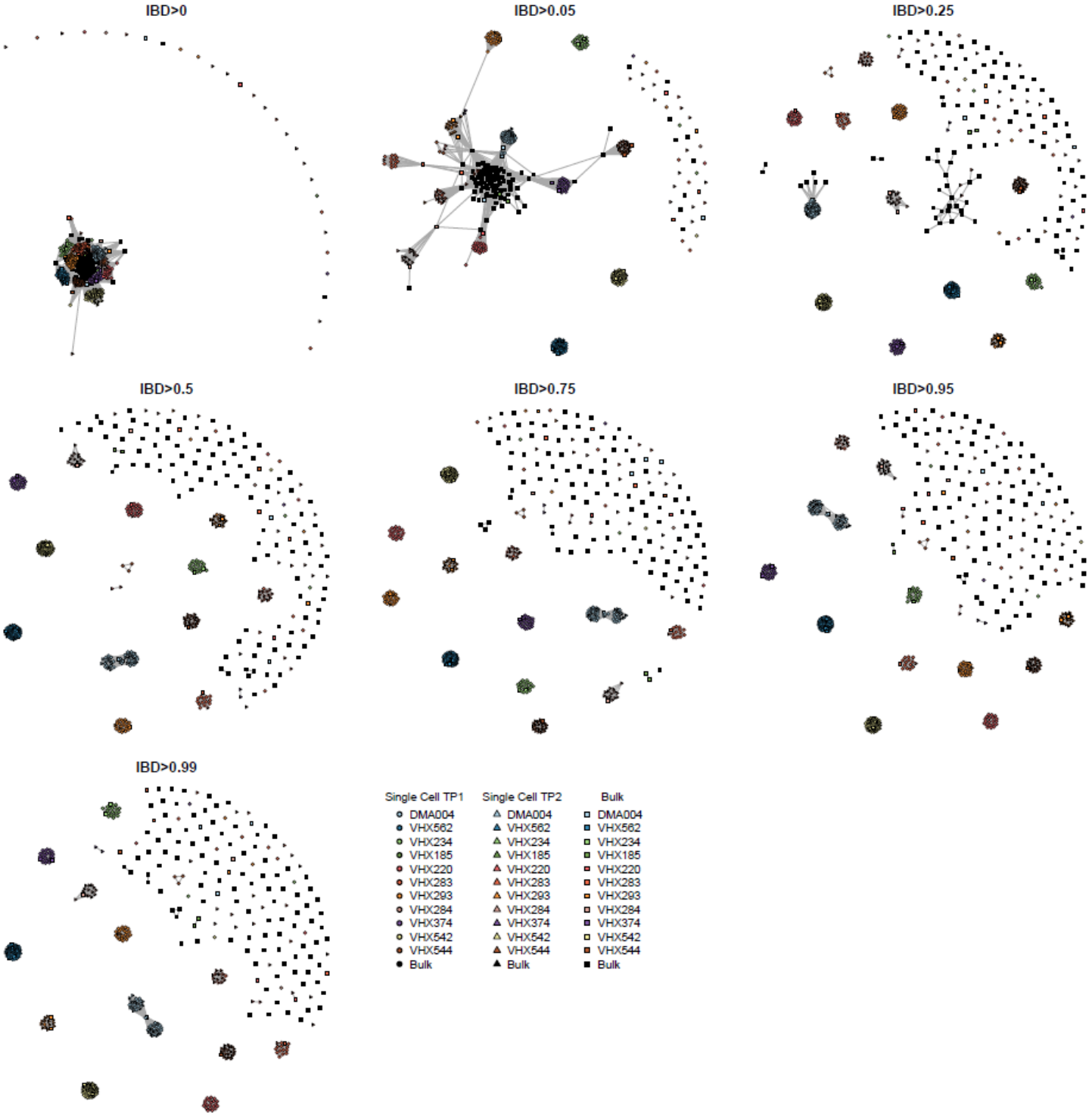

Fig. S2. Network analysis of identity by descent using progressive thresholds, related to Figure 2.

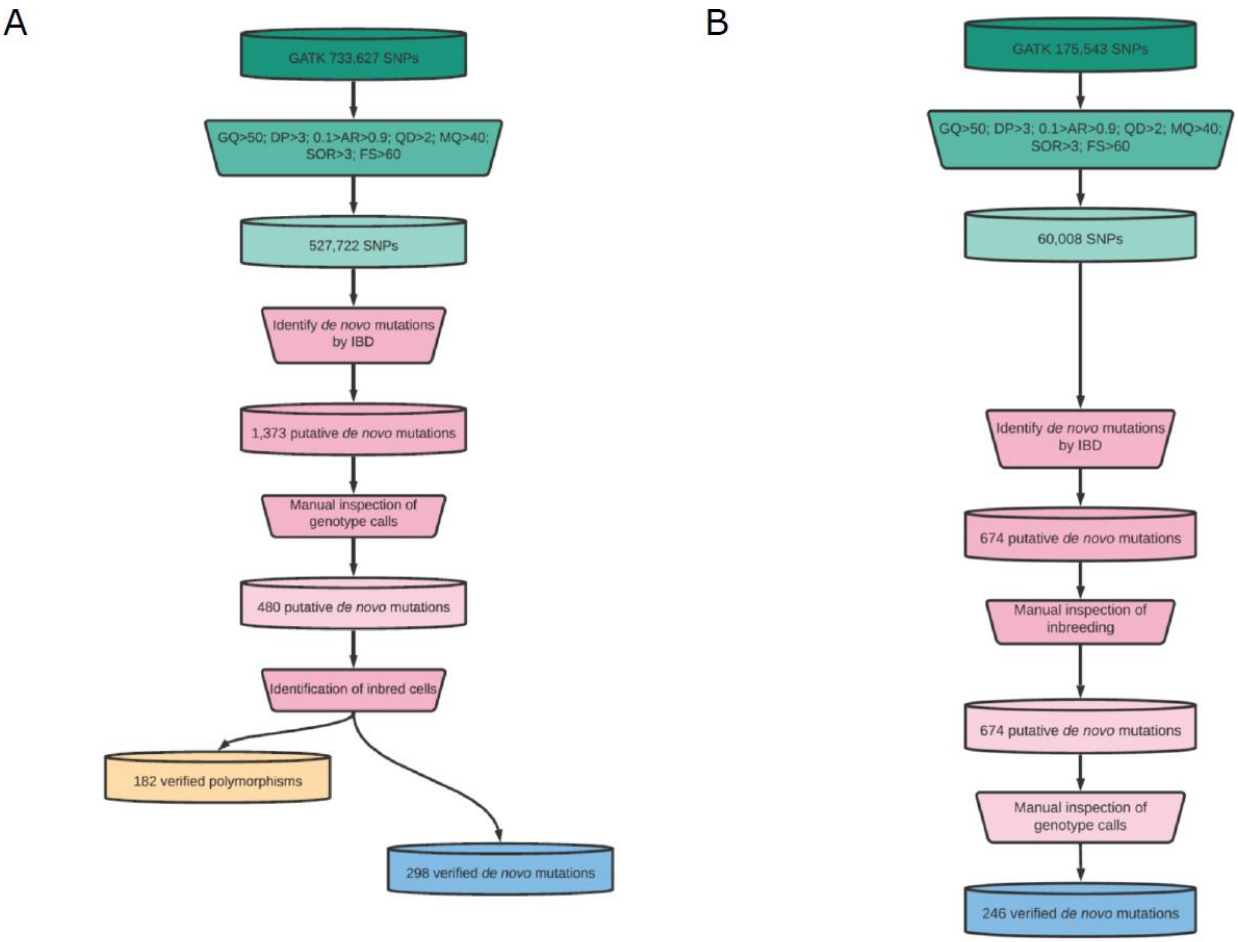

Fig. S3. A flow chart depicting the identification and quality control of de novo SNPs identified in *P. vivax* infections (A) and *P. falciparum* infections (B), Related to STAR Methods.

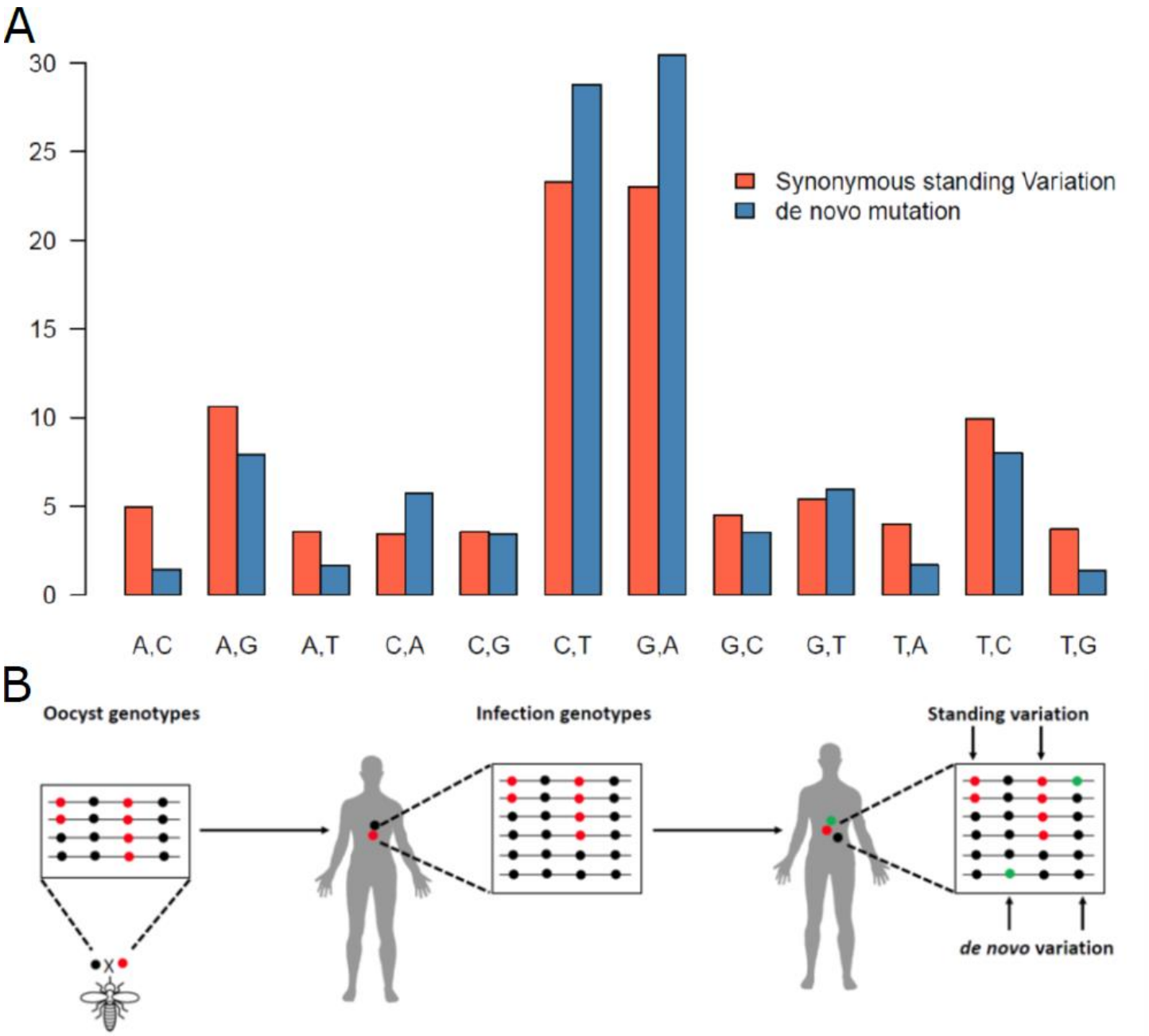

Fig. S4. Identification of putative de novo mutations, related to STAR Methods and Figure 3. Minimal bias in the ratio of different base pair changes supports low error rate from lysis induced mutations (A). We compared the difference between the distribution of mutational classes of synonymous mutation (which minimizes the impact of selection on the mutational process) to the mutations we identified as putative de novo mutations using a chi squared test (p=0.745, chi=7.6, df=11). A definition of standing and *de novo* variation (B).

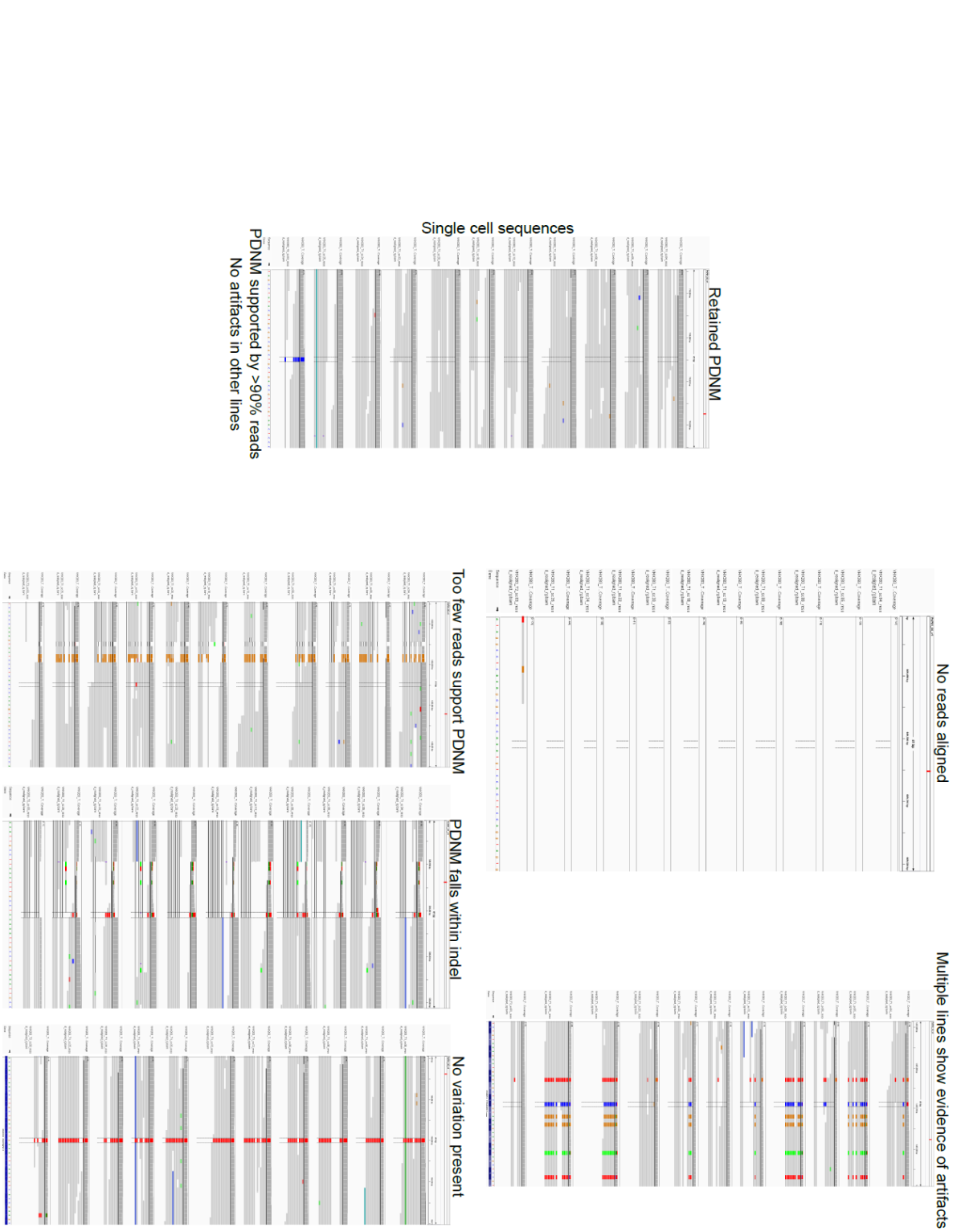

Fig S5. Examples of identification of errors in putative de novo mutations, related to STAR Methods.

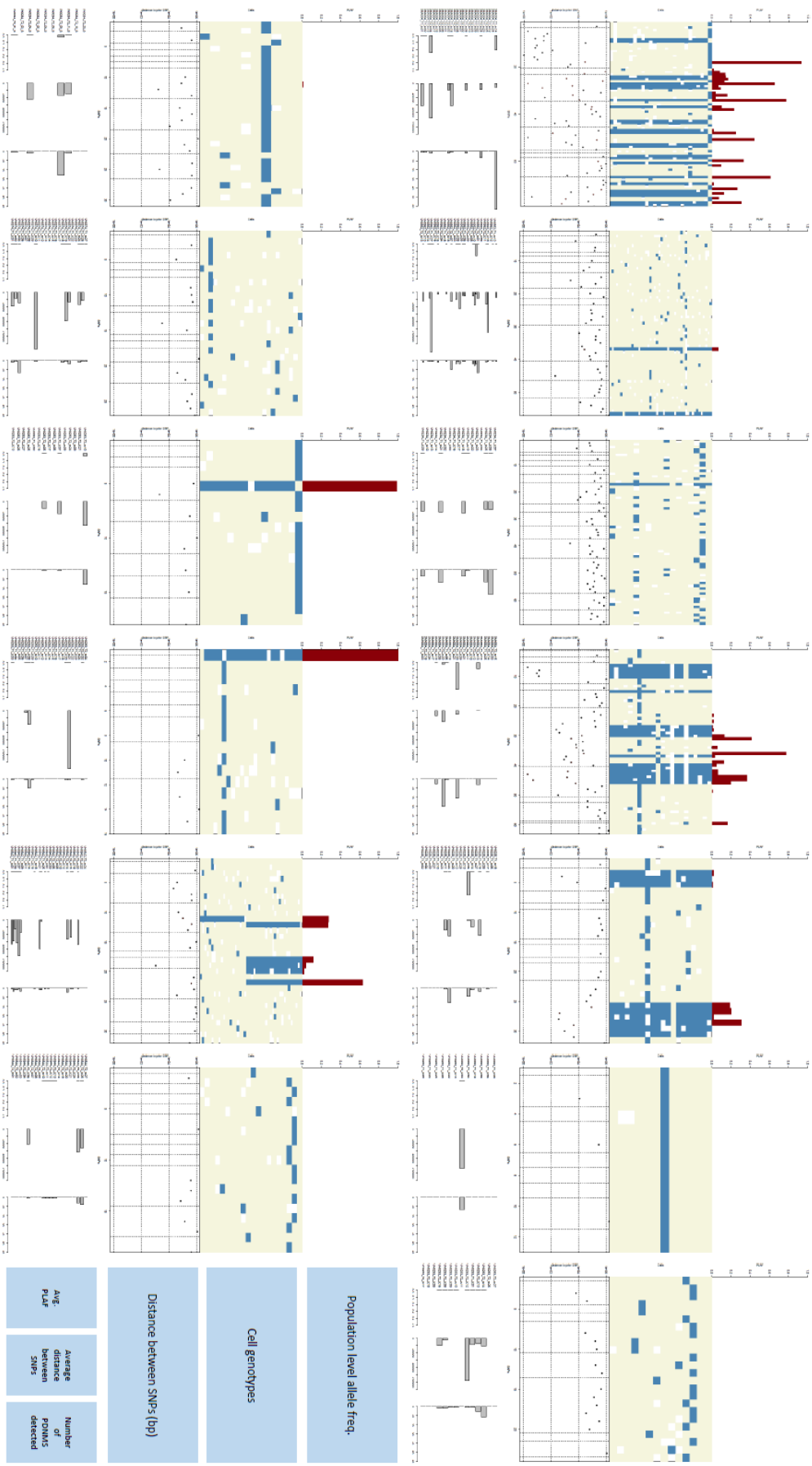
Avg. PLAF
Average distance between SNPs
Number of PDNMS detected
Distance between SNPs (bp)
Cell genotypes
Population level allele freq.

Fig S6. Identification of inbreeding events in *P. vivax* single cell data, related to Figure 3. The data depicted in each group of panels is shown in the lower right. For each group identified by IBD we show the population level allele frequency (PLAF) of the alternative allele (top), the genotype of each cell (second from top), the distance between consecutive PDNMs (third from top). The lowest group of panels show the average PLAF in PDNMs specific to the cell (lower left), the average distance between PDNMs specific to the cell (lower middle) and the number of PDMNs detected (lower right). The cell names are shown next to the lower group of panels. Cells with an average PLAF of >0 or >30 PDNMs detected were classified as likely driven by inbreeding, this was corroborated by examining the distribution of distance between PDMNs specific to the cell.

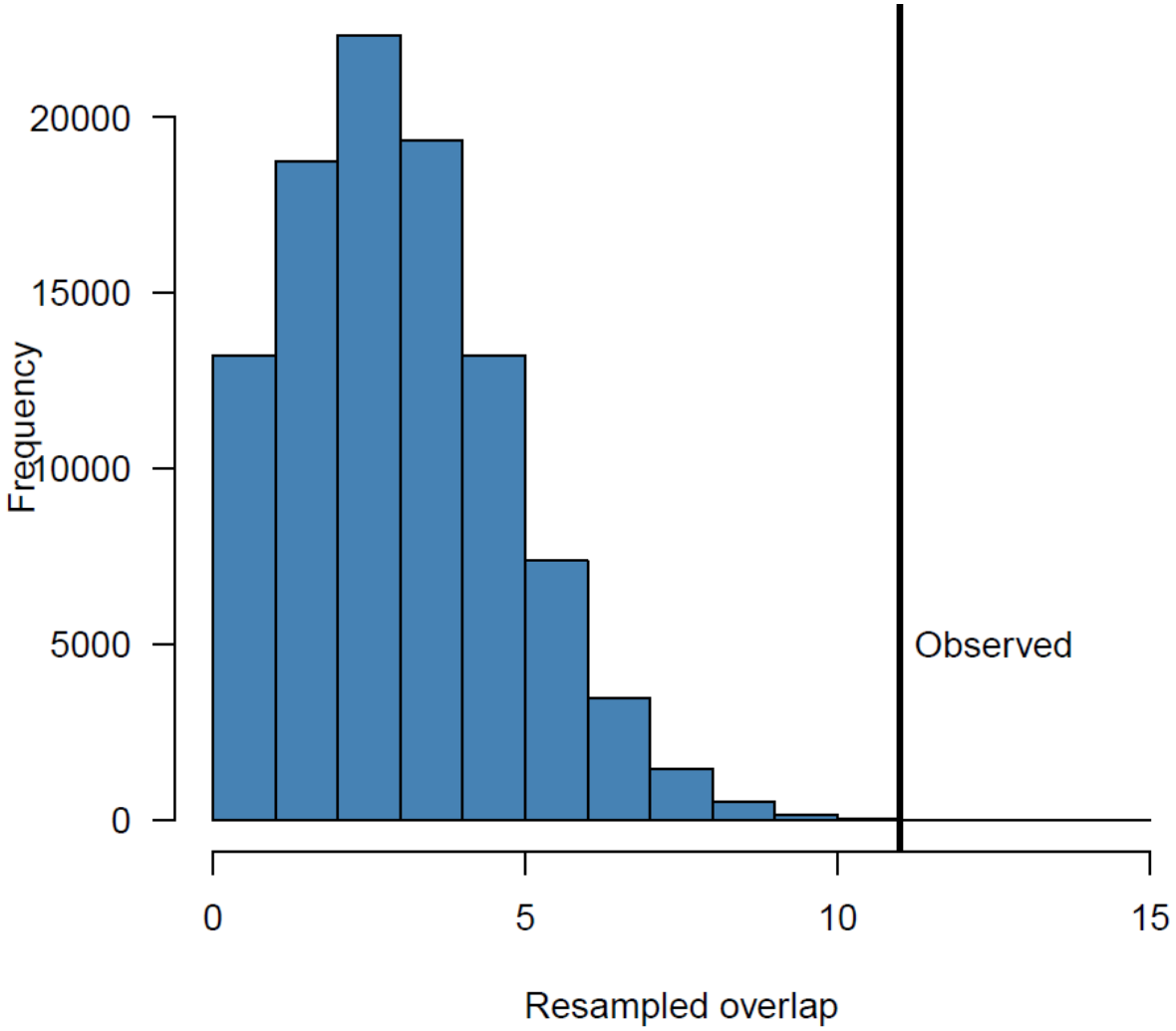

Fig. S7. Bootstrap resampling of the distribution of overlapping genes expected when drawing orthologous genes bearing *de novo* mutations between *P. vivax* and *P. falciparum*, related to Table 2.

Study	Code	Date	Days between events	Pregnant	Primary	Age	Sex	Location	pv1000/RBC	Bulk	Sorted RBCs	Single Cells
VHX	185	6/25/2010		non-pregnant	primary inf	32	UNK	MKT	7	1	0	0
VHX	185	8/27/2010	63	non-pregnant	UNK	32	UNK	MKT	5	1	0	0
VHX	220	8/19/2010		non-pregnant	UNK	27	F	MKT	2	0	1	24
VHX	220	10/21/2010	63	non-pregnant	UNK	25	F	MKT	2	0	1	24
VHX	234	7/19/2010		non-pregnant	primary inf	42	F	Wangpa	2	1	1	21
VHX	234	5/19/2011	304	non-pregnant	previous malaria	42	F	Wangpa	2	0	0	0
VHX	283	11/16/2010		non-pregnant	reinfection	4	M	Wangpa	4	1	1	24
VHX	283	1/4/2011	49	non-pregnant	primary inf	4	M	Wangpa	2	1	1	24
VHX	284	8/24/2010		non-pregnant	primary inf	27	F	Wangpa	3	1	0	6
VHX	284	12/23/2010	121	non-pregnant	reinfection	27	F	Wangpa	10	1	0	23
VHX	293	8/27/2010		non-pregnant	reinfection	15	M	Wangpa	3	1	1	24
VHX	293	8/4/2011	342	non-pregnant	primary inf	15	M	Wangpa	5	1	1	22
VHX	374	10/5/2010		non-pregnant	primary inf	20	M	Maela	2	1	1	24
VHX	374	5/23/2011	230	non-pregnant	UNK	20	M	Maela	2	1	1	18
VHX	542	7/6/2011		non-pregnant	primary inf	17	M	Maela	2	1	1	22
VHX	542	9/16/2011	72	non-pregnant	UNK	17	M	Maela	8	1	1	24
VHX	544	8/4/2011		non-pregnant	primary inf	11	F	MKT	3	0	1	9
VHX	544	12/9/2011	127	non-pregnant	previous malaria	11	F	MKT	2	1	1	21
VHX	562	8/4/2011		non-pregnant	primary inf	13	M	MKK,PLU	2	1	1	22
VHX	562	1/21/2012	170	non-pregnant	primary inf	13	M	MKK,PLU	5	1	1	24
DMA	004	9/14/2010		pregnant	reinfection	32	F	Wangpa	5	1	1	24
DMA	004	10/13/2010	29	pregnant	reinfection	32	F	Wangpa	2	1	1	24

Table S1. Information on the patients and infections sampled in this study, related to STAR Methods.

Identifier	p-value	FDR corrected p value	Pathway	pathway_source_id
GO:0001522	3.00E-03	0.00072	pseudouridine synthesis	GO
LIPA-CORESYN-PWY	0.00021	0.001575	Lipid A-core biosynthesis	MetaCyc
PWY-5469	0.00018	0.001575	sesamin biosynthesis	MetaCyc
PWY-7250	0.00032	0.0016	2Fe-2Siron-sulfur cluster biosynthesis	MetaCyc
ec00231	0.00142	0.005325	Puromycin biosynthesis	KEGG
PWY-7650	0.00196	0.00588	echinocandin B biosynthesis	MetaCyc
COA-PWY-1	0.0032	0.008	coenzyme A biosynthesis II (mammalian)	MetaCyc
ec00230	0.00465	0.00845	Purine metabolism	KEGG
PWY-7559	0.00507	0.00845	glutathione degradation (DUG pathway - yeast)	MetaCyc
CYCLOHEXANOL-OXIDATION-PWY	0.00416	0.00845	cyclohexanol degradation	MetaCyc
BENZCOA-PWY	0.00565	0.008475	anaerobic aromatic compound degradation (Thauera aromatica)	MetaCyc
ANAEROFRUCAT-PWY	0.00847	0.01155	homolactic fermentation	MetaCyc
PWY-4702	0.01169	0.0146125	phytate degradation I	MetaCyc
GO:0006468	0.00297	0.02784	protein phosphyloation	GO
GO:0016021	0.00348	0.02784	integral component of membrane	GO

Table S4. Pathway and GO term enrichment of *de novo* mutations, related to Table 2.

Patient	Days	Months	Unrelated	Clonal	Related and Unrelated	All Related	pop. prob. Reinfection (Taylor et al)
DMA004	29	0.97				Y	0
VHX283	49	1.63			Y		0.05
VHX185	63	2.1	NA	NA	NA	NA	0.06
VHX220	63	2.1			Y		0.06
VHX542	72	2.4		Y			0.07
VHX284	121	4.03				Y	0.1
VHX544	127	4.23			Y		0.11
VHX562	170	5.67		Y			0.13
VHX374	230	7.67			Y		0.15
VHX234	304	10.13	NA	NA	NA	NA	0.2
VHX293	342	11.4			Y		0.25

Table S5. Comparison between the IBD patterns within infections and estimates the subsequent infection was due to reinfection using microsatellite data from Taylor *et al*, related to Figure 2.